Mathematical Modeling of the Central Carbohydrate Metabolism in Arabidopsis Reveals a Substantial Regulatory Influence of Vacuolar Invertase on Whole Plant Carbon Metabolism[1][W]

Thomas Nägele, Sebastian Henkel, Imke Hörmiller, Thomas Sauter, Oliver Sawodny, Michael Ederer, and Arnd G. Heyer*

Biologisches Institut, Abteilung Botanik (T.N., I.H., A.G.H.), and Institut für Systemdynamik (S.H., O.S., M.E.), Universität Stuttgart, D–70550 Stuttgart, Germany; and Life Science Research Unit, Université du Luxembourg, L–1511 Luxembourg (T.S.)

A mathematical model representing metabolite interconversions in the central carbohydrate metabolism of Arabidopsis (*Arabidopsis thaliana*) was developed to simulate the diurnal dynamics of primary carbon metabolism in a photosynthetically active plant leaf. The model groups enzymatic steps of central carbohydrate metabolism into blocks of interconverting reactions that link easily measurable quantities like CO_2 exchange and quasi-steady-state levels of soluble sugars and starch. When metabolite levels that fluctuate over diurnal cycles are used as a basic condition for simulation, turnover rates for the interconverting reactions can be calculated that approximate measured metabolite dynamics and yield kinetic parameters of interconverting reactions. We used experimental data for Arabidopsis wild-type plants, accession Columbia, and a mutant defective in vacuolar invertase, AtβFruct4, as input data. Reducing invertase activity to mutant levels in the wild-type model led to a correct prediction of increased sucrose levels. However, additional changes were needed to correctly simulate levels of hexoses and sugar phosphates, indicating that invertase knockout causes subsequent changes in other enzymatic parameters. Reduction of invertase activity caused a decline in photosynthesis and export of reduced carbon to associated metabolic pathways and sink organs (e.g. roots), which is in agreement with the reported contribution of vacuolar invertase to sink strength. According to model parameters, there is a role for invertase in leaves, where futile cycling of sucrose appears to have a buffering effect on the pools of sucrose, hexoses, and sugar phosphates. Our data demonstrate that modeling complex metabolic pathways is a useful tool to study the significance of single enzyme activities in complex, nonintuitive networks.

During the last few years, systems biology has become a rapidly expanding interdisciplinary field of research, driven by the need to study complex interactions among components of biological systems (Yuan et al., 2008). Basically, the intention of systems biology is to resolve the relationship between individual entities (e.g. molecules or genes that are part of highly interconnected networks) in order to understand the resulting system behavior (e.g. a phenotype of an organism). To handle complex networks, formal representation by mathematical models is combined with the integration of experimental data for gene expression, protein abundance, metabolite concentration, or other biological parameters. In an iterative process of model development and experimental validation, systems biology will advance system-wide understanding of complex biological networks (Stelling, 2004). The aim of this study was to use experimentally determined steady-state levels of metabolites, measured at various time points over a complete diurnal cycle, to model fluxes of metabolite interconversions, which are difficult to assess at high time resolution. This is achieved by generating a set of differential equations that represent changes in metabolite levels caused by the interconverting reactions.

Representation of biological processes by differential equations has successfully been applied at various levels of biological complexity in plants. Light and dark reactions of photosynthesis have been modeled, and steady-state concentrations of metabolites and electron transport rates could be predicted (Pettersson and Ryde-Pettersson, 1988; Laisk et al., 2006). The Calvin cycle reactions of photosynthesis have been modeled, and flux control coefficients were determined for individual enzymes (Poolman et al., 2000). The circadian clock of Arabidopsis (*Arabidopsis thaliana*) was modeled using differential equations for interlocked dynamics in the abundance of transcrip-

[1] This work was supported by Landesstiftung Baden-Württemberg (grant no. 33–729.64–3/28 to A.G.H. [project A6] and O.S. [project C]) in the frame of the Center Systems Biology at the University of Stuttgart.

* Corresponding author; e-mail arnd.heyer@bio.uni-stuttgart.de.

The author responsible for distribution of materials integral to the findings presented in this article in accordance with the policy described in the Instructions for Authors (www.plantphysiol.org) is: Arnd G. Heyer (arnd.heyer@bio.uni-stuttgart.de).

[W] The online version of this article contains Web-only data.

www.plantphysiol.org/cgi/doi/10.1104/pp.110.154443

tion factors and participating components (Locke et al., 2005, 2006). Furthermore, kinetic modeling was applied to elucidate the factors governing Suc accumulation in sugarcane (*Saccharum officinarum*; Uys et al., 2007). Mathematical modeling can also be applied to investigate the consequences of gene knockouts and is especially useful when mutated genes are part of complex networks that prevent intuitive understanding of the consequences of individual gene failure. For example, in aliphatic glucosinolate synthesis, knockouts in one of several methylthioalkylmalate synthases generate varying patterns of glucosinolate chain lengths. Simulations using kinetic models revealed that chain length distribution is a function of the ratio, not of absolute activities, of different methylthioalkylmalate synthases (Knoke et al., 2009).

A prominent example of a complex network that, because of branching and metabolite cycling, is no longer traceable by intuition is the central carbohydrate metabolism in plants. As immediate products of photosynthesis, carbohydrates are the most important energy source as well as building blocks for the synthesis of other organic materials. In addition, they are involved in the regulation of fundamental processes like cell division, growth, differentiation, and resource allocation in plants (Koch, 1996; Smeekens, 2000). In the model plant Arabidopsis as well as in many other plant species, starch and Suc represent the main primary products of photosynthesis (Caspar et al., 1985; Geiger et al., 2000; Gibon et al., 2004b).

Hydrolytic cleavage of Suc into hexose monomers is catalyzed by invertase (EC 3.2.1.26) that occurs as three different isoenzymes, vacuolar invertase, cell wall-bound invertase, and neutral invertase, which can be distinguished based on their subcellular localization, solubility, and pH optima (Sturm, 1999; Roitsch and Gonzalez, 2004). While biochemical properties and molecular details of invertases are well known, their importance in plant carbohydrate metabolism is not fully understood. We demonstrate here that mathematical modeling can be employed to investigate the physiological role of vacuolar invertases in carbohydrate metabolism of a plant leaf. Based on measured metabolite levels and CO_2-exchange rates, the model computes kinetic parameters for interconverting reactions in order to simulate experimentally determined metabolite dynamics. To reduce complexity, individual enzymatic steps can be combined into blocks of interconversions that directly link the metabolites that have been quantified. In this case, kinetic parameters do not represent individual enzymes but consecutive interconverting steps. The model calculates turnover rates for the metabolites, which cannot be assessed directly from steady-state levels, when branch points or cycles appear in a metabolic pathway. We used modeling of Arabidopsis accession Columbia (Col-0) with artificially reduced invertase activity to emulate a knockout of the main vacuolar invertase, AtβFruct4 (At1G12240), to investigate whether effects of the knockout could be predicted. In parallel, we developed a model based on experimental data for the mutant. Comparison of the simulations revealed consequences of invertase knockout for consecutive enzymatic steps.

RESULTS

Model States: Carbon Fixation, Starch Accumulation, and Suc Turnover

For modeling, we used a simplified scheme of central carbohydrate metabolism that concentrates on the most abundant sugars and sugar phosphates as important intermediates at which pathways branch (Fig. 1). The model does not resolve subcellular compartments, because we aimed at minimizing complexity in order to increase unambiguousness of simulations. Thus, the aerial organs of a vegetative plant are collectively treated as the source that assimilates carbon and, to some extent, exports assimilates to sinks. Sink export as displayed in Figure 1 is a combination of sugar transport to heterotrophic organs and export of assimilated carbon into metabolic pathways not included in the scheme (e.g. synthesis of cell wall material, amino acids, and others). We use the term "combined sink export" to differentiate it from Suc transport to sink organs.

In this system, dynamics in sugars are afforded by simple inputs and outputs (i.e. CO_2 assimilation, respiration, and combined sink export) as well as by changes in system states (i.e. levels of metabolites). As a prerequisite for modeling the diurnal dynamics, these model states were measured.

Based on three consecutive recordings, mean diurnal CO_2-exchange profiles were generated as representative for plants in the 14-leaf stage (Fig. 2, wild type). From these profiles, rates of photosynthesis during the day and respiration during the night were calculated. Under the growing conditions in a greenhouse with natural light supplemented to a minimum of 80 μmol photons m^{-2} s^{-1}, we reproducibly obtained a steep increase in CO_2 uptake during the first 3 h of the light phase, a drop around midday, and a linear decline after a second peak around 2 PM (Fig. 2, 14:00).

In parallel to the wild type, recordings were done for the *inv4* mutant defective in vacuolar invertase gene At1g12240, which was later used for comparison. Note that significant differences for diurnal dynamics of carbon fixation rates were obtained between the genotypes: peak values of fixation rates were similar but were reached about 1 h later in the mutant. Accordingly, the increase in fixation rate during the first 3 h after light-on was faster in the wild type. After reaching the peak value, CO_2 fixation rate showed a faster decline in *inv4*, resulting in slightly lower fixation rates. At night, *inv4* showed markedly higher respiration rates than the wild type.

Diurnal patterns of transitory starch metabolism were similar in the wild type and *inv4*, with continuous but decreasing rates of starch accumulation during the light phase and a nocturnal breakdown following a

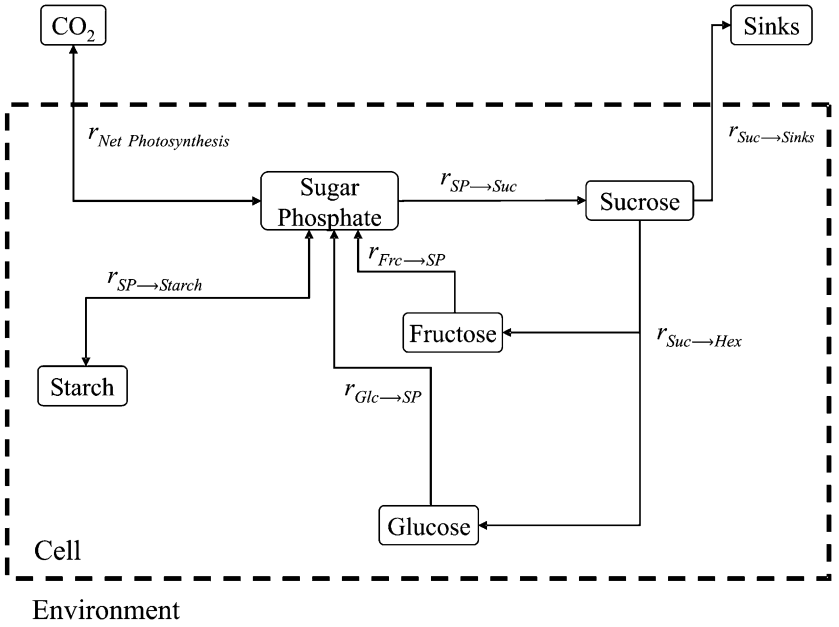

Figure 1. Schematic representation of the primary carbohydrate metabolism of plant leaf cells. Reaction rates (r) represent central processes of carbon input, output, and interconversion. Frc, Fructose.

similar course (Fig. 3). Starch content did not change markedly during the first 3 h of the light phase, and accumulation rates were maximal between 9 AM and 6 PM, before slowing down between 6 and 10 PM. Within the first hour in the dark (10–11 PM), starch content of both genotypes decreased rapidly from about 16 to 10 μmol C_6 g^{-1} fresh weight, followed by a slowdown of the degradation rate until the end of the night.

Simulation of Central Carbohydrate Metabolism

Next, we developed a mathematical model of the central carbohydrate metabolism based on a set of six ordinary differential equations that represented the concentrations of sugar phosphates, Suc, Glc, Fru, starch, and the combined sink export, such that all metabolite interconversions given in Figure 1 were included as terms of the ordinary differential equations. Metabolite interconversions in this model can be composite reactions that include multiple enzymatic steps, as in the case for sugar phosphate and Suc synthesis, the latter involving phosphoglucoisomerase, UDP-Glc pyrophosphorylase, Suc-P synthase (SPS), and Suc-P phosphatase, while the former summarizes the entire Calvin cycle. Additionally, membrane transport events may be included (e.g. during Suc hydrolysis, where invertase isoforms in the vacuole and the apoplast have to be considered). Assuming that all sugar interconversions have a rate-limiting step depending on a catalyst (e.g. an enzyme or transporter), we used Michaelis-Menten kinetics for modeling. In the case of Suc hydrolysis ($r_{\mathrm{Suc}\rightarrow\mathrm{Hex}}$) and

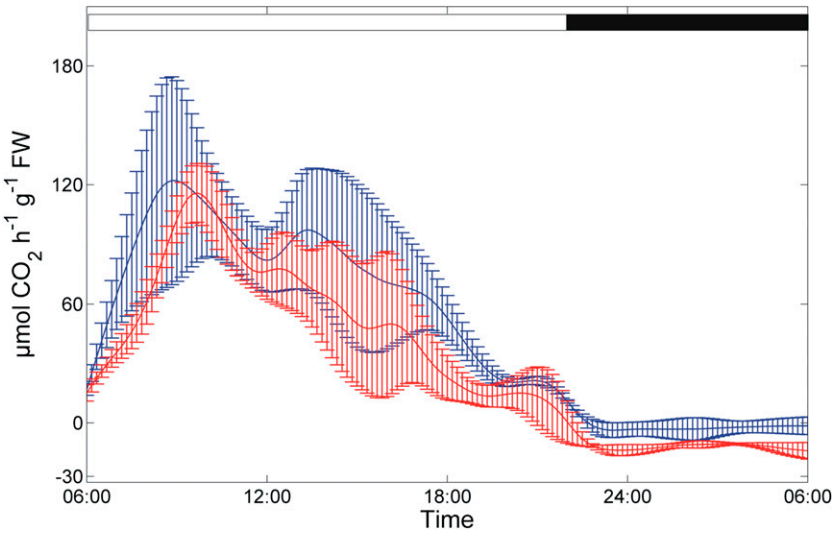

Figure 2. Diurnal rates of net photosynthesis of wild-type (blue) and *inv4* knockout (red) plants. The day/night transition is indicated by the white and black bars at top. Solid lines represent the interpolation of means from three measurements ± SD. FW, Fresh weight.

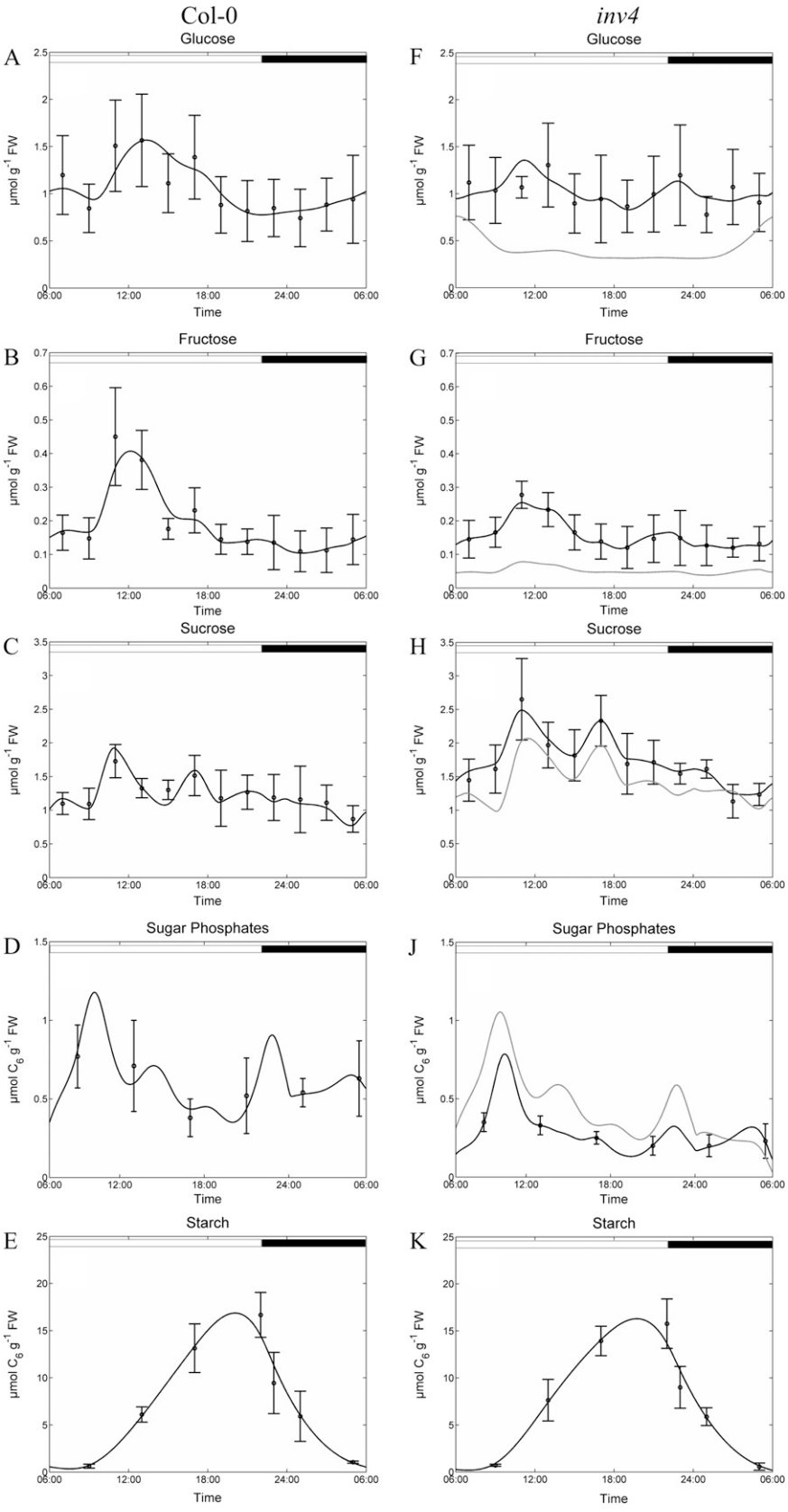

Figure 3. Diurnal dynamics of central carbohydrates in leaf cells of wild-type plants (A–E) and *inv4* mutant plants (F–K). Day/night transitions are indicated by white and black bars at top. Black circles represent means of measurements ± SD ($n = 8$). Black lines represent results of model simulations. Gray lines represent results of model simulations of Col-0 with invertase activities of *inv4*. Diurnal starch accumulation was interpolated as indicated by black lines in E and K. FW, Fresh weight.

phosphorylation of hexoses ($r_{Fru \rightarrow SP}$ and $r_{Glc \rightarrow SP}$), product inhibition was considered as described (Sturm, 1999; Claeyssen and Rivoal, 2007). Based on data from the literature, the rate-limiting step for Suc synthesis was assumed to be the reaction of SPS, which by phosphorylation is regulated at the level of V_{max} (Huber and Huber, 1992). Since V_{max} is dynamic in the model, no additional level of regulation was required. In contrast to sugar levels, measured rates of photosynthesis and starch buildup were implemented as immediate reaction rates (for detailed model structure, see "Materials and Methods"), because no branching or cycling occurred in these parts of the network.

Simulations using measured metabolite levels as a frame of reference adjust kinetic parameters of interconverting reactions such that dynamics in metabolite levels can be approximated. The simulations incorporate the role of each metabolite as product or substrate in all model reactions. The output of simulations are kinetic parameters from which flux rates of interconversions can be calculated when substrate concentrations are included. In the simplified model depicted in Fig. 1, all interconversions are substrate reactions, which are irreversible, because all contain at least one irreversible step, so that the route from educt to product cannot be reversed even if the rate-limiting step is a reversible reaction. In a pathway that contains branch points or cycles, this allows the identification of partitioning between subbranches, which in our case is the distribution of assimilates (i.e. sugar phosphates) between combined export, transitory starch metabolism, and Suc cycling.

We measured concentrations of Suc, Fru, and Glc as well as Glc-6-P and Fru-6-P as the dominant constituents of the sugar phosphate pool over a complete diurnal cycle. These data were fed into the model together with net photosynthesis and starch accumulation rates. The rationale behind feeding metabolite levels into model simulations is that this allows the calculation of flux parameters based on steady-state measurements, which is not possible without modeling. In an iterative process of simulating metabolite concentrations and reaction rates, and minimizing deviations between calculated and measured model states, dynamics of five metabolite concentrations and eight reaction rates are modeled over a 24-h diurnal cycle.

For all metabolites, simulated dynamics in the wild type (Fig. 3, left) fell within the SD of the quantification, thus affirming the authenticity of the model output. Obvious differences in measured metabolite levels between the wild type and the *inv4* mutant are the substantially higher dynamics of hexoses in the wild type and the elevated Suc concentration in the mutant. Suc concentrations in the mutant and the wild type significantly ($P < 0.05$) deviated during the entire light phase but not during the night, while the hexose-to-Suc ratio differed between the two genotypes from late morning to afternoon (11 AM–7 PM). Simulated flux rates for the wild type (Figs. 4 and 5) indicated that the majority of assimilates are exported, accounting for at least 70% of fixed carbon. Consequently, the pattern of Suc export was tightly coupled to the simulated assimilation rate (Fig. 4; $r_{Photosynthesis}$ and $r_{Suc \rightarrow Sinks}$). In contrast, export was not strictly dependent on the Suc concentration, pointing to some regulatory instance controlling export. Comparison of the rates for Suc synthesis and export revealed a ratio of about 1.4 in the morning, which increased in the afternoon when export faded. This implies that Suc was subject to turnover within the source organs in a futile cycle of breakdown and rebuild operated by invertase, hexokinase/fructokinase, and the enzymes involved in Suc synthesis, which together constitute $r_{SP \rightarrow Suc}$.

Validation of Model Simulations

As a first step in the validation of model simulations, we determined V_{max} of the rate-limiting steps of interconverting reactions at 5 AM (i.e. 1 h prior to light on), 1 PM (7 h into the 16-h light phase), and 9 PM (1 h before light off) and compared these with values from the simulations (Table I). All simulated V_{max} levels fell within the SD of quantification.

To prove the usefulness of the simulation, we then tested whether the knockout in vacuolar invertase activity could be simulated by artificially reducing

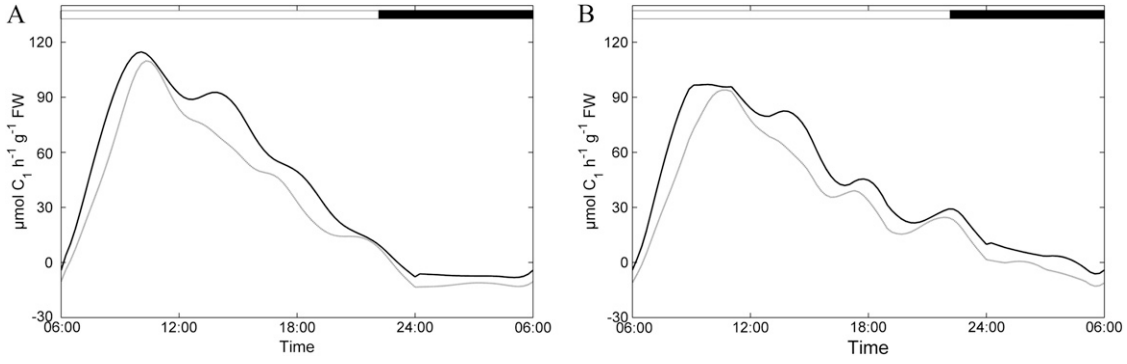

Figure 4. Simulated diurnal dynamics of rates of net photosynthesis (A) and sink export (B) for the wild type (black lines) and *inv4* (gray lines). Day/night transitions are indicated by white and black bars at top. FW, Fresh weight.

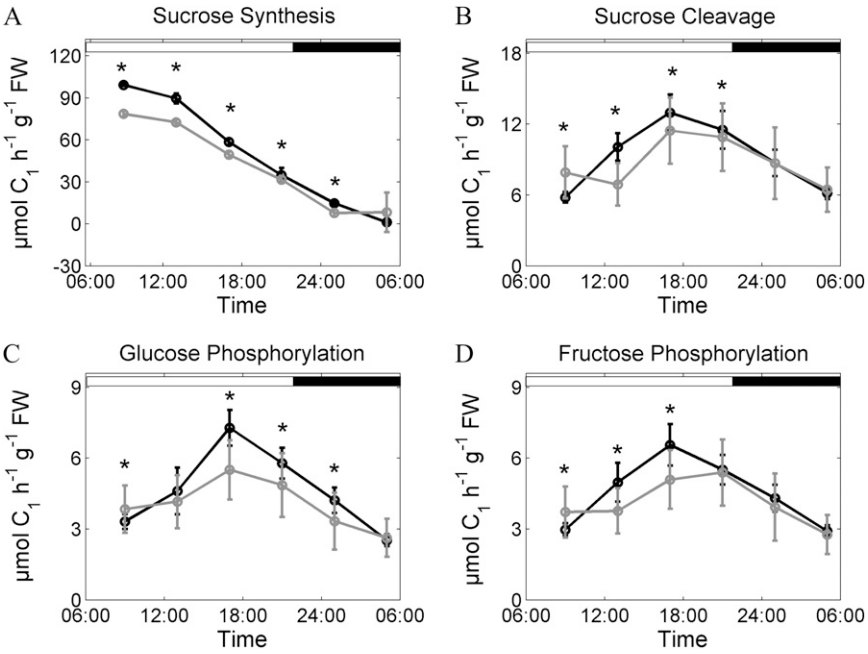

Figure 5. Diurnal dynamics of simulated rates of Suc synthesis (A), Suc cleavage (B), Glc phosphorylation (C), and Fru phosphorylation (D). Simulation results are represented for the wild type (black lines) and the *inv4* knockout mutant (gray lines). Circles represent means of simulations ± SD (n = 75). Asterisks indicate significant differences from the wild type ($P <$ 0.01). FW, Fresh weight.

invertase activity of the wild type to mutant levels. As a prerequisite for this approach, V_{max} levels of invertase were quantified over the whole diurnal cycle (Fig. 6). V_{max} of vacuolar invertase in the wild type showed strong diurnal fluctuation with a steep increase until midday, followed by a constant decrease until the end of the night. Neutral cytoplasmic invertase reached 20% to 30% of vacuolar invertase until noon but was very low thereafter, while cell wall invertase peaked in the evening, reaching about half of V_{max} of vacuolar invertase. Due to the knockout of the dominant vacuolar invertase, the corresponding V_{max} was very low in *inv4* plants. Interestingly, V_{max} of cell wall invertases was also strongly reduced in *inv4* plants, while dynamics were unchanged. Neutral invertase made up about half of the activity in *inv4*, with V_{max} for total invertase being reduced to one-tenth of the wild type.

The in silico knockout of vacuolar invertase makes the assumption that an individual gene knockout reduces the maximum turnover rate (V_{max}) of the respective metabolite interconversion with no consequences for other reactions, which is not necessarily the case. However, our simulations using the wild-type model with invertase activity intentionally reduced to 10% approximately produced Suc levels measured for the mutant (Fig. 3H, gray line). Simulations of sugar phosphates yielded values intermediate between the wild type and the mutant; however, simulated hexose levels were much lower than determined for the mutant. This indicates changes in kinetic parameters of interconverting reactions inevitably resulting from the reduction in invertase activity, which discriminates the mutant from the wild type. The fact that deviations from quantifications occurred in metabolites downstream of invertase points to modifications in hexokinase activity (see below).

Comparison of Independent Models for the Wild Type and the *inv4* Mutant

Because the in silico knockout of vacuolar invertase led to simulated metabolite levels deviating from quantifications, we performed an independent parameter identification for the mutant entirely based on metabolite levels determined for this genotype. The simulations for *inv4* and the wild type were replicated 75 times to allow statistical analysis of the identified kinetic parameters. The results of these simulations are summarized in Table II. As expected, K_m and K_i values for the wild type and mutant were not significantly different, except for the K_m of $r_{SP\rightarrow Suc}$ and the K_i of invertase. All values were in agreement with values taken from the literature. The reduction of K_m for $r_{SP\rightarrow Suc}$ probably reflects the reduced sugar phosphate concentration in the mutant, which negatively influences the affinity of SPS for Fru-6-P (Doehlert and Huber, 1983). The difference in K_i for invertase is a result of the change in the dominating form of invertase in the mutant (see below).

The mutant displayed reduced reaction rates for Suc synthesis, Suc cleavage, and hexose phosphorylation over the entire light phase, but this reduction was significant only in the case of Suc synthesis (Fig. 5). This reflects the reduction in photosynthesis and combined sink export determined for the mutant (Fig. 4) and points to a role of invertase for sink strength.

Interestingly, flux through invertase in source leaves was significantly reduced only at midday, when hexose levels peaked in the wild type, but caught up when Suc hydrolysis was highest in the afternoon (Fig. 5B). Another interesting feature was a slight increase of Suc cleavage and hexose phosphorylation during the night, which correlates with the elevated night

Table I. *Validation of enzyme parameters determined by parameter estimation*

Values of K_m and K_i are given in mM. The unit of maximum enzyme activity (V_{max}) is μmol h^{-1} g^{-1} fresh weight. F6P, Fru-6-P; FrcK, fructokinase; G6P, Glc-6-P; GlcK, glucokinase; Inv, invertase.

Reaction	Parameter	Genotype	Parameter Estimation	Experimental Data	Literature Values		
					Value	Species	Reference
$r_{SP\rightarrow Suc}$ (SPS)	V_{max} (5 AM)	Col-0	0.4 ± 0.2	3.7 ± 3.6	32.4	Arabidopsis	Gibon et al. (2004a)
		inv4	3.9 ± 6.8	5.5 ± 0.9			
	V_{max} (1 PM)	Col-0	27.1 ± 1.4	30.2 ± 5.1			
		inv4	21.9 ± 1.0	23.8 ± 4.0			
	V_{max} (9 PM)	Col-0	12.2 ± 1.3	9.6 ± 4.1			
		inv4	12.3 ± 1.3	8.8 ± 2.9			
	K_m	Col-0	0.53 ± 0.082	–	0.7–0.8	*Spinacia oleracea*	Harbron et al. (1981)
		inv4					
$r_{Suc\rightarrow Hex}$ (Inv)	V_{max} (5 AM)	Col-0	68.0 ± 6.9	59.3 ± 18.4	60	Arabidopsis	Klotke et al. (2004)
		inv4	11.0 ± 0.001	7.9 ± 3.2			
	V_{max} (1 PM)	Col-0	155.5 ± 12.0	137.0 ± 29.0			
		inv4	12.9 ± 0.2	8.6 ± 4.9	30,000		Tang et al. (1996)
	V_{max} (9 PM)	Col-0	99.9 ± 7.5	114.7 ± 20.6			
		inv4	17.0 ± 1.8	15.6 ± 4.3			
	K_m	Col-0	11.7 ± 1.21	–	5–12	Arabidopsis	Tang et al. (1996)
		inv4					
	$K_{i,Glc}$	Col-0	0.01 ± 0.001	–	–	–	–
		inv4					
	$K_{i,Fru}$	Col-0	0.78 ± 2.29	–	2.5	*Lolium temulentum*	Kingston-Smith et al. (1999)
		inv4					
$r_{Fru\rightarrow SP}$ (FrcK)	V_{max} (5 AM)	Col-0	4.1 ± 0.5	4.61 ± 1.31	5.0 ± 0.5	Arabidopsis	Moore et al. (2003)
		inv4	4.9 ± 1.6	5.0 ± 0.4			
	V_{max} (1 PM)	Col-0	3.6 ± 0.6	4.0 ± 0.8			
		inv4	4.4 ± 1.2	3.1 ± 0.8			
	V_{max} (9 PM)	Col-0	8.0 ± 1.3	9.2 ± 0.4			
		inv4	8.8 ± 2.6	7.8 ± 1.9			
	K_m	Col-0	0.8 ± 0.075	–	1.5–30	*S. oleracea*	Claeyssen and Rivoal (2007)
		inv4					
	$K_{i,F6P}$	Col-0	1.97 ± 0.31	–	–	–	–
		inv4					
$r_{Glc\rightarrow SP}$ (GlcK)	V_{max} (5 AM)	Col-0	4.8 ± 0.9	4.8 ± 1.3	3.8 ± 0.2	Arabidopsis	Moore et al. (2003)
		inv4	4.5 ± 1.5	4.1 ± 0.4			
	V_{max} (1 PM)	Col-0	6.2 ± 1.7	3.4 ± 1.6			
		inv4	5.2 ± 1.5	3.8 ± 0.1			
	V_{max} (9 PM)	Col-0	12.9 ± 2.8	10.1 ± 1.9			
		inv4	7.9 ± 2.4	8.6 ± 0.4			
	K_m	Col-0	0.1 ± 0.02	–	0.02–0.13	*S. oleracea*	Claeyssen and Rivoal (2007)
		inv4					
	$K_{i,G6P}$	Col-0	0.14 ± 0.03	–	No effect	*Pisum sativum*	Claeyssen and Rivoal (2007)
		inv4			Weak effect	*Zea mays*	

respiration of *inv4*. Together, these effects abolished the morning rise of Suc cleavage appearing in the wild type and explain the absence of a clear hexose peak in the mutant. In contrast to the in silico mutation of vacuolar invertase, the *inv4* model afforded a reduction in hexokinase activity, and this allowed stabilization of hexose pools as well as alignment of measured and simulated sugar phosphate levels.

Surprisingly, Suc cycling was not significantly reduced in the *inv4* mutant in spite of the lack of the dominating vacuolar invertase. A comparison of V_{max} of total invertase and flux at different time points (Table II) shows that flux reaches about 2% of V_{max} in the wild type and about 30% in *inv4*. This implies that flux of Suc hydrolysis did not reach the upper bound (i.e. V_{max} of invertase activity in either genotype). However, it is important to note that, at given K_m and K_i values and nearly constant Suc concentrations, as found in the wild type (Fig. 3C), modulations of V_{max} are essential to create hexose dynamics. This is demonstrated by the in silico invertase mutation, where hexose dynamics are damped down.

DISCUSSION

Dynamic Simulation of Central Carbohydrate Metabolism

Diurnal turnover of key metabolites like soluble sugars and starch is difficult to measure, because

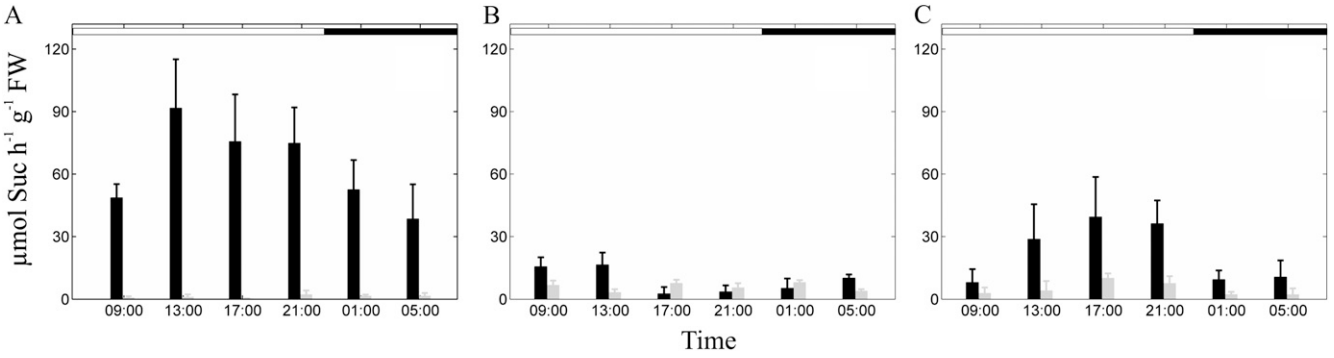

Figure 6. Diurnal activities of vacuolar (A), neutral (B), and cell wall-bound (C) invertase in wild-type (black bars) and *inv4* knockout (gray bars) plants. Results represent means ± SD ($n = 5$). FW, Fresh weight.

determination of flux rates using labeling techniques is very laborious, thus creating a tradeoff between high time resolution and statistical robustness. Dynamic simulation integrating quantitative data for metabolites to identify kinetic parameters in metabolic networks is an attractive alternative to flux measurement and has successfully been applied to model metabolic pathways in yeast (Rizzi et al., 1997; Theobald et al., 1997). Kinetic modeling is widely used to simulate metabolite dynamics based on known kinetic parameters of enzymes (Poolman et al., 2004). We chose a different strategy and used data on diurnal dynamics of metabolite levels to identify kinetic parameters of the interconverting reactions. As a frame of reference for simulating central carbohydrate metabolism of a photosynthetically active leaf of Arabidopsis, metabolite levels of samples taken over a complete diurnal cycle were determined. Exchange of CO_2 served as input into, and a combined export to, sink organs as well as to other metabolic pathways as modeled output from the system. Metabolites linking input and output were quantified and fed into the simulations as model states. Sugars and starch did not accumulate in the leaves during the first 3 h of the light phase, although maximal CO_2 fixation occurred within this interval. This caused the simulated combined export to peak within the first 3 h of the day, and the following decline of export coincided with an accumulation of soluble sugars and starch in the leaf. From this pattern, it is evident that reduced export triggered a pileup of carbohydrates in the leaf. This was affirmed by the *inv4* mutant, which lacks the dominant vacuolar invertase and is characterized by a reduced Suc turnover in roots that causes lowered sink strength (Sergeeva et al., 2006). Due to the reduced Suc demand in sinks, soluble sugars increased in leaves of *inv4* and photosynthesis was lower. Repression of photosynthesis as a consequence of sugar and/or starch accumulation in mature source leaves under sink limitation is a well-known phenomenon (Le et al., 2001; Kasai et al., 2008) and can explain the lower photosynthetic rate of *inv4*. The diurnal pattern of photosynthetic activity and carbohydrate levels in the wild type as well as *inv4*, however, demonstrated that this phenomenon not only occurs as a medium- or long-term effect but as a regular consequence of daily photosynthesis. Pool sizes for soluble sugars and starch in leaves are small compared with photosynthetic input; thus, the buffering capacity of a leaf is limited. The fact that photosynthesis was reduced already after the morning peak points to a fast negative feedback regulation. Evidence for a rapid regulatory effect on photosynthesis has been obtained for culms of sugarcane, where Suc feeding caused significantly lower assimilation and electron transport rates already within 2 h (McCormick et al., 2008). This inhibition can indeed occur regularly under normal growth conditions because of source overcapacity, as demonstrated for greenhouse-grown tomato (*Solanum lycopersicum*) plants, where midday depression of photosynthesis was stronger in spring than in winter because of the higher light intensities (Ayari et al., 2000).

Under growth conditions with moderate light intensity, we found that the Suc concentration in the leaves was relatively stable in wild-type plants. Considering the large variation in sink export that closely followed the pattern of photosynthesis, this shows that export was not directly dependent on leaf Suc concentration and that the Suc concentration was to some extent buffered. In contrast, Suc was fairly dynamic in *inv4*, probably due to a combination of reduced turnover in sink as well as in source organs, which caused net accumulation. One possibility of stabilizing the Suc pool in leaves would be the futile cycling of Suc breakdown and rebuild, which was postulated 20 years ago to be a constitutive pathway controlling cellular Suc levels (Huber, 1989). Its contribution to flux through Suc was calculated as 17% to 30% based on the accumulation rate of hexoses in girdled soybean (*Glycine max*) leaves (Huber, 1989). Uys et al. (2007) determined its contribution to Suc turnover to be 22% in culms of sugarcane. This is in agreement with our simulations, where cycling contributed 10% to 25% of Suc synthesis in the wild type during the light phase. Under conditions of reduced sink demand, cycling should increase in sources in order to stabilize the Suc

Table II. *Diurnal dynamics of identified enzyme parameters represented in the model*

Values of K_m and K_i are given in mM. The unit of maximum enzyme activity (V_{max}) is μmol h^{-1} g^{-1} fresh weight. Asterisks indicate significant differences from the wild type (* $P < 0.01$, ** $P < 0.001$).

Genotype	Reaction	Parameter	Time					
			9 AM	1 PM	5 PM	9 PM	1 AM	5 AM
Col-0	$r_{SP\rightarrow Suc}$	V_{max}	27.9 ± 1.8	27.1 ± 1.4	21.9 ± 2.2	12.2 ± 1.3	4.8 ± 0.3	0.4 ± 0.2
	K_m: 0.53 ± 0.082							
	$r_{Suc\rightarrow Hex}$	V_{max}	68.3 ± 8.1	155.5 ± 12.0	141.6 ± 12.1	99.9 ± 7.5	70.2 ± 5.5	68.0 ± 6.9
	K_m: 11.7 ± 1.21							
	$K_{i,Glc}$: 0.01 ± 0.001							
	$K_{i,Fru}$: 0.78 ± 2.29							
	$r_{Fru\rightarrow SP}$	V_{max}	3.5 ± 0.5	3.6 ± 0.6	7.9 ± 1.3	8.0 ± 1.3	8.1 ± 1.4	4.1 ± 0.5
	K_m: 0.8 ± 0.075							
	K_i: 1.97 ± 0.31							
	$r_{Glc\rightarrow SP}$	V_{max}	6.1 ± 1.0	6.2 ± 1.7	12.4 ± 2.6	12.9 ± 2.8	10.27 ± 2.3	4.83 ± 0.9
	K_m: 0.1 ± 0.02							
	K_i: 0.14 ± 0.03							
inv4	$r_{SP\rightarrow Suc}$	V_{max}	23.1 ± 1.0*	21.9 ± 1.0*	17.0 ± 1.2*	12.3 ± 1.3	3.0 ± 1.1*	3.9 ± 6.8
	K_m: 0.27 ± 0.02							
	$r_{Suc\rightarrow Hex}$	V_{max}	12.9 ± 0.2**	12.9 ± 0.2**	15.0 ± 0.001**	17.0 ± 1.8**	11.8 ± 1.3**	11.0 ± 0.001**
	K_m: 8.12 ± 2.74							
	$K_{i,Glc}$: 0.07 ± 0.06							
	$K_{i,Fru}$: 1.9 ± 4							
	$r_{Fru\rightarrow SP}$	V_{max}	5.8 ± 1.8*	4.4 ± 1.2*	9.5 ± 2.8	8.8 ± 2.6	7.1 ± 2.5*	4.9 ± 1.6
	K_m: 1.17 ± 0.27							
	K_i: 2.16 ± 0.47							
	$r_{Glc\rightarrow SP}$	V_{max}	6.0 ± 1.8	5.2 ± 1.5*	9.5 ± 2.8*	7.9 ± 2.4*	6.7 ± 2.3*	4.5 ± 1.5
	K_m: 0.08 ± 0.02							
	K_i: 0.147 ± 0.016							

pool. However, in *inv4*, this appears to be constrained and thus Suc accumulates.

There are several reports on the putative regulatory role of Suc cycling for photosynthetic activity (Goldschmidt and Huber, 1992; Krapp et al., 1993; Moore et al., 1998). These studies are in favor of a negative impact of a high flow through hexokinase on the expression of photosynthetically relevant genes, based on observations that, under conditions of sink limitation or feeding of exogenous sugars, expression of the gene for the small subunit of Rubisco is downregulated. However, in an investigation on regulatory events during leaf development in Arabidopsis, Stessman et al. (2002) demonstrated that the period of high photosynthetic activity and expression of chlorophyll *a*/*b*-binding protein of the light-harvesting complex (*Lhcb*) coincided with a constantly increasing rate of assimilate partitioning into hexoses. At later stages, when flux into Suc was still high but flux into hexose declined, *Lhcb* transcripts were strongly reduced and photosynthetic activity dropped steeply. This agrees with our observation that high Suc-to-hexose ratios were correlated with lowered photosynthetic activity in wild-type and *inv4* plants. In this context, it is interesting to compare our in silico mutation of invertase with the invertase model based on measurements for the mutant. This revealed that solely reducing V_{max} of invertase in the wild type drained the hexose pool to levels even lower than those found in the mutant. Modeling the mutant yielded a reduction of hexokinase in conjunction with reduced invertase activity, which stabilized the hexose pool. This strongly suggests that the cell responds to lowered invertase activity in order to prevent drainage of hexoses.

Starch is often considered as an overflow product of photosynthesis in plants with insufficient sink demand or assimilate transport capacity (Eichelmann and Laisk, 1994; Komor, 2000). Alternatively, it has been suggested that starch synthesis is bimodal, with an overflow as well as a programmed component that is constitutive for plants growing in a day/night regime (Sun et al., 1999). We found similar dynamics for starch in the wild type and *inv4*, arguing for a large contribution of the constitutive component under our growth conditions. The absolute levels of starch, which were substantially lower than reported for plants in high light (Gibon et al., 2004b), are in favor of this interpretation. However, low levels of starch and low-light conditions seem to conflict with the above-mentioned midday repression of photosynthesis resulting from sink limitation and pileup of carbohydrates in the sources, when source capacity and sink strength are regarded as static system properties. From our simulations that revealed photosynthesis and sink export to be tightly linked, we conclude that sink demand and export activity are interlaced (i.e. daily consumption of assimilates by sink organs is adjusted to the prevailing source capacity and, in turn, constrains photosynthesis at peak levels). The lower sink strength in invertase mutants thus caused generally

lower assimilation, but maximum photosynthetic rates are still beyond the bounds of consumption, so that sink limitation becomes a regular daily phenomenon and plays an important role in sink/source communication.

The Physiological Role of Vacuolar Invertase

Diurnal measurement of net photosynthetic rates for wild-type plants and *inv4* mutants revealed a delayed start of photosynthesis and down-regulation in the afternoon as well as elevation of leaf respiration in *inv4* during the night. The lowered photosynthesis in the afternoon could have arisen from the reported negative effect of the invertase knockout on sink strength (Sergeeva et al., 2006) or, conversely, could be the cause of reduced export. Two lines of evidence point to the former: (1) at all time points except in the middle of the night, total leaf sugar in *inv4* was higher than in the wild type (Fig. 3), thus making reduced substrate availability for export unlikely; and (2) respiratory activity of leaves was higher in *inv4* during the dark period, pointing to an overaccumulation of assimilates in leaves (Fig. 2).

While the effects on afternoon photosynthesis and night respiration can thus be attributed to reduced sink strength, the delayed rise of carbon assimilation in the morning more likely reflects an effect of vacuolar invertase on leaf metabolism. We found a strong reduction in the pool of sugar phosphates in *inv4* especially in the night and the early morning. Sugar phosphates were fairly constant between 0.5 and 1 μmol g^{-1} fresh weight over the day in the wild type, which is in agreement with data from the literature (Strand et al., 1997). However, in *inv4* the pool size was substantially reduced, particularly in the morning, when photosynthesis commenced operation. Considering that Calvin cycle intermediates are part of this pool, this would explain the delayed start of photosynthesis in the *inv4* mutant and indicates a role of Suc cycling and, hence, of leaf invertase in controlling sugar phosphate pools. While functions of invertase have clearly been demonstrated for growth-related processes in juvenile petioles of sugar beet (*Beta vulgaris*; Gonzalez et al., 2005) or tobacco (*Nicotiana tabacum*) seedlings (Bonfig et al., 2007), a role in adult plants is still elusive. Recently, antisense suppression of soluble acid invertase in muskmelon (*Cucumis melo*) has revealed destructive effects on chloroplast ultrastructure that point to an involvement in the regulation of primary photosynthetic processes and would agree with a role in stabilizing sugar phosphate pools (Yu et al., 2008).

Apart from reduced sink strength, increased Suc concentrations in leaves of *inv4* could directly contribute to reduced photosynthetic activity. In fact, Suc levels are higher at all time points during the light phase in the mutant. Inhibition of photosynthesis by carbohydrates accumulating in the mesophyll cells has been described for plants with reduced assimilate transport capacity because of an inhibition of the Suc transporter (Riesmeier et al., 1994), an inhibition of Suc loading into the phloem due to expression of a pyrophosphatase in companion cells (Geigenberger et al., 1996), or by cold girdling of the petiole (Krapp et al., 1993). In this context, it is interesting to speculate on the measured decline of cell wall invertase activity in *inv4* plants. Although we cannot exclude a pleiotropic effect of the knockout mutation, an alternative interpretation is intriguing. We observed highest cell wall invertase activities in wild-type plants during afternoon, following a strong reduction of sink export at around 2 PM. If phloem loading is considered the driving force of assimilate transport, reduced export from the mesophyll would have an inhibitory feed-forward effect because of reduced metabolic activity in companion cells, as has been demonstrated (Lerchl et al., 1995). Cell wall invertases can compensate this by increasing the Suc gradient between mesophyll and apoplast, thereby increasing hexose supply to companion cells. Because Suc concentration in leaves of *inv4* plants is strongly elevated while sink strength is low, induction of cell wall invertase to sustain the gradient might be unneeded and, in turn, induction of cell wall invertase might fail.

Taken together, our mathematical simulation of leaf carbohydrate metabolism allows the evaluation of sets of flux rates in a complex metabolic network and provides insights into metabolite partitioning at metabolic branch points. Using the *inv4* mutant, which shows significant but nondramatic alterations in primary metabolism, the technique proves high sensitivity and allows for evaluation of the role of a single enzyme that is embedded in a complex metabolic network.

MATERIALS AND METHODS

Plant Material

Arabidopsis (*Arabidopsis thaliana*) plants used in this study were grown in GS90 soil and vermiculite (1:1) with three plants per 10-cm pot in a growth chamber at 8 h of light (55 μmol m^{-2} s^{-1}; 22°C)/16 h of dark (16°C) for 4 weeks and then transferred to a greenhouse with a 22°C day (16 h) and a 16°C night (8 h) temperature regime. In the greenhouse, natural light was supplemented to an intensity of at least 80 μmol m^{-2} s^{-1} by incandescent lamps from 6 AM to 10 PM, and relative humidity was 70%. Plants were watered daily and fertilized every 2 weeks with standard nitrogen-phosphorus-potassium fertilizer. Leaf samples consisting of two rosette leaves each were taken every 2 h over a complete day/night cycle from nine individual plants gown in three different pots in a random design 6 weeks after sowing (i.e. shortly before bolting). At that stage, the aerial part of the plant is exclusively composed of rosette leaves, allowing a direct comparison of metabolite and CO_2-exchange data. Leaf samples were weighed, immediately frozen in liquid nitrogen, and stored at –80°C until metabolite extraction.

Gas-Exchange Measurements

Exchange rates of CO_2 were measured using an infrared gas analysis system (Uras 3 G; Hartmann & Braun). A whole-rosette cuvette design was used similar to that described by Kollist et al. (2007). Plexiglass cylinders were applied instead of stainless steel. The cylinders were sealed to the lower surface of a rectangular plexiglass plate with transparent and vacuum-tight joint grease (Buddeberg Laboratory Technology). Gas exchange was measured

at 3 consecutive days in the greenhouse shortly before plant harvest over whole day (16-h)/night (8-h) cycles. Means of raw data for gas exchange were converted to flux rates per gram fresh weight obtained at the end of the exposure by weighing complete rosettes.

Carbohydrate Analysis

Frozen leaf samples were homogenized using a ball mill (MM20; Retsch). The homogenate was extracted twice in 400 μL of 80% ethanol at 80°C. Extracts were dried and dissolved in 500 μL of distilled water. Contents of Glc, Fru, and Suc were analyzed by high-performance anion-exchange chromatography using a CarboPac PA-1 column on a Dionex DX-500 gradient chromatography system coupled with pulsed amperometric detection by a gold electrode.

Concentrations of Glc-6-P and Fru-6-P were determined as described by Gibon et al. (2002).

For starch extraction, pellets of the ethanol extraction were solubilized by heating them to 95°C in 0.5 N NaOH for 30 min. After acidification with 1 N CH_3COOH, the suspension was digested for 2 h with amyloglucosidase. The Glc content of the supernatant was then determined and used to assess the starch content of the sample.

Measurement of Enzyme Activities

Enzyme activities were determined in crude extracts of leaf samples. To assess activities of soluble acid invertase, cell wall-bound invertase and neutral invertase, about 100 mg of frozen leaf tissue, were homogenized in 50 mM HEPES-KOH (pH 7.4), 5 mM $MgCl_2$, 1 mM EDTA, 1 mM EGTA, 1 mM phenylmethylsulfonyl fluoride, 5 mM dithiothreitol (DTT), 0.1% Triton X-100, and 10% glycerin. Suspensions were centrifuged at 6,000 rpm for 25 min at 4°C, and invertase activities were assayed in the supernatants. Soluble acid invertase was assayed in 20 mM Na-acetate buffer (pH 4.7) using 100 mM Suc as substrate. Neutral invertase was assayed in 20 mM HEPES-KOH (pH 7.5) also using 100 mM Suc as substrate. Activity of cell wall-bound invertase was determined as described for soluble acid invertase without centrifugation of the homogenized suspension and subsequent subtraction of soluble acid invertase activity. The control of each assay was boiled for 3 min after the addition of enzyme extract. Reactions were incubated for 60 min at 30°C and stopped by boiling for 3 min, and the concentration of Glc was determined photometrically (Pharmacia).

Activity of SPS was determined following the method of Huber et al. (1989). After homogenizing frozen leaf tissue in 50 mM HEPES-KOH (pH 7.5), 15 mM $MgCl_2$, 1 mM EDTA, 2.5 mM DTT, and 0.1% Triton X-100, the suspension was centrifuged at 13,000 rpm for 5 min at 4°C and SPS activity was assayed in the supernatant using a reaction buffer consisting of 50 mM HEPES-KOH (pH 7.5), 15 mM $MgCl_2$, 2.5 mM DTT, 10 mM UDP-Glc, 10 mM Fru-6-P, and 40 mM Glc-6-P, which is an activator of SPS. Thirty percent KOH was added to the control of each assay. Reactions were incubated for 30 min at 25°C, followed by an incubation for 10 min at 95°C. Anthrone (0.2%) in 95% H_2SO_4 was added, and the samples were incubated for 8 min at 90°C. Glc concentration was determined photometrically at a wavelength of 620 nm.

Activity of glucokinase and fructokinase was determined as described (Wiese et al., 1999). Synthesized Glc-6-P was converted to 6-phosphogluconolactone by Glc-6-P dehydrogenase and could be measured photometrically by changes in concentration of the reduced cosubstrate NADPH. For isomerization of Fru-6-P, which was synthesized by fructokinase, 1.75 units of phosphoglucoisomerase was added, and the formed Glc-6-P could be determined as described for glucokinase.

Modeling and Simulation

A mathematical model was developed representing the central carbohydrate metabolism in leaves of Arabidopsis. The model was based on the following system of ordinary differential equations describing time-dependent alterations in carbohydrate pools:

$$d/dt(\mathrm{SP}) = \tfrac{1}{6} r_{\mathrm{NetPhotosynthesis}} - r_{\mathrm{SP}\rightarrow\mathrm{Starch}} - r_{\mathrm{SP}\rightarrow\mathrm{Suc}} + r_{\mathrm{Fru}\rightarrow\mathrm{SP}} + r_{\mathrm{Glc}\rightarrow\mathrm{SP}}$$
$$d/dt(\mathrm{Starch}) = r_{\mathrm{SP}\rightarrow\mathrm{Starch}}$$
$$d/dt(\mathrm{Suc}) = \tfrac{1}{2} r_{\mathrm{SP}\rightarrow\mathrm{Suc}} - \tfrac{1}{2} r_{\mathrm{Suc}\rightarrow\mathrm{Sinks}} - r_{\mathrm{Suc}\rightarrow\mathrm{Hex}}$$
$$d/dt(\mathrm{Glc}) = r_{\mathrm{Suc}\rightarrow\mathrm{Hex}} - r_{\mathrm{Glc}\rightarrow\mathrm{SP}}$$
$$d/dt(\mathrm{Fru}) = r_{\mathrm{Suc}\rightarrow\mathrm{Hex}} - r_{\mathrm{Fru}\rightarrow\mathrm{SP}}$$
$$d/dt(\mathrm{Sinks}) = r_{\mathrm{Suc}\rightarrow\mathrm{Sinks}}$$

These state equations for sugar phosphates (SP), starch, Suc, Glc, Fru, and combined sink export (Sinks) depended on the adjoining fluxes [$r(t)$]. The different $r_{\mathrm{A}\rightarrow\mathrm{B}}$ describe the respective metabolic fluxes from metabolite A to metabolite B (Fig. 1).

The rate of net photosynthesis ($r_{\mathrm{Net\ Photosynthesis}}$) was approximated by a smoothing spline interpolation of measurements over whole diurnal cycles. Rates of starch synthesis and breakdown were determined by interpolation of measurements and calculating the first derivative of this function. These rates were fed into the model as a reversible reaction rate ($r_{\mathrm{SP}\rightarrow\mathrm{Starch}}$), assuming that both processes are connected to the pool of sugar phosphates. The rate of combined Suc export ($r_{\mathrm{Suc}\rightarrow\mathrm{Sinks}}$) was calculated as the difference between the rate of net photosynthesis and the rate of changes in the carbohydrate pools.

All other fluxes were modeled as irreversible Michaelis-Menten enzyme kinetics:

$$r_{\mathrm{A}\rightarrow\mathrm{B}}(t) = \frac{V_{\mathrm{max,A}} \times c_{\mathrm{A}}(t)}{K_{\mathrm{m,A}} + c_{\mathrm{A}}(t)}$$

At this, the reaction rate $r_{\mathrm{A}\rightarrow\mathrm{B}}(t)$ depends on substrate concentration $c_{\mathrm{A}}(t)$, maximum activity of the catalyzing enzyme ($V_{\mathrm{max,A}}$), and the enzyme-specific substrate affinity, expressed by $K_{\mathrm{m,A}}$.

Values of V_{max} were considered adjustable during diurnal cycles, whereas values of K_{m} were defined to be constant. A possible diurnal modulation of substrate affinity in the reactions $r_{\mathrm{Suc}\rightarrow\mathrm{Hex}}$, $r_{\mathrm{Glc}\rightarrow\mathrm{SP}}$, and $r_{\mathrm{Fru}\rightarrow\mathrm{SP}}$ was incorporated via concentration changes of allosteric effectors, which were considered as follows: the reaction rate of Suc cleavage (enzyme: invertase) was modeled as an irreversible Michaelis-Menten enzyme kinetic incorporating mixed inhibition by the products Glc and Fru. Glc was modeled as a noncompetitive inhibitor and Fru as a competitive inhibitor (Sturm, 1999). Reaction rates of Glc and Fru phosphorylation (enzyme: hexokinase) were modeled as Michaelis-Menten enzyme kinetics noncompetitively inhibited by sugar phosphates (Claeyssen and Rivoal, 2007).

The identification of unknown parameters was carried out by minimizing the cost function (i.e. the sum of squared errors between simulated and measured states) by variation of the model parameters. The identification process was performed using a particle-swarm pattern search method for bound constrained global optimization as described (Vaz and Vicente, 2007).

The model was implemented in the numerical software Matlab (version 7.6.0.324, R2008a) using the software packages Systems Biology Toolbox2 and the SBPD Extension Package as described (Schmidt and Jirstrand, 2006). The model files and the optimization procedure are available as Supplemental Data Files S1 to S4.

Statistics

All *t*-tests were performed using the software Matlab (version 7.6.0.324, R2008a).

Supplemental Data

The following materials are available in the online version of this article.

Supplemental Data File S1. Model Col-0.

Supplemental Data File S2. Model *inv4*.

Supplemental Data File S3. Optimization procedure Col-0.

Supplemental Data File S4. Optimization procedure *inv4*.

ACKNOWLEDGMENT

We thank Annika Allinger for excellent plant cultivation.

Received February 4, 2010; accepted March 3, 2010; published March 5, 2010.

LITERATURE CITED

Ayari O, Dorais M, Gosselin A (2000) Daily variations of photosynthetic efficiency of greenhouse tomato plants during winter and spring. J Am Soc Hortic Sci **125:** 235–241

Bonfig KB, Berger S, Fatima T, Gonzalez MC, Roitsch T (2007) Metabolic control of seedling development by invertases. Funct Plant Biol **34:** 508–516

Caspar T, Huber SC, Somerville C (1985) Alterations in growth, photosynthesis, and respiration in a starchless mutant of *Arabidopsis thaliana* (L.) deficient in chloroplast phosphoglucomutase activity. Plant Physiol **79:** 11–17

Claeyssen E, Rivoal J (2007) Isozymes of plant hexokinase: occurrence, properties and functions. Phytochemistry **68:** 709–731

Doehlert DC, Huber SC (1983) Regulation of spinach leaf sucrose phosphate synthase by glucose-6-phosphate, inorganic phosphate and pH. Plant Physiol **73:** 989–994

Eichelmann H, Laisk A (1994) CO_2 uptake and electron transport rates in wild-type and a starchless mutant of *Nicotiana sylvestris*. Plant Physiol **106:** 679–687

Geigenberger P, Lerchl J, Stitt M, Sonnewald U (1996) Phloem-specific expression of pyrophosphatase inhibits long-distance transport of carbohydrates and amino acids in tobacco plants. Plant Cell Environ **19:** 43–55

Geiger DR, Servaites JC, Fuchs MA (2000) Role of starch in carbon translocation and partitioning at the plant level. Aust J Plant Physiol **27:** 571–582

Gibon Y, Blaesing OE, Hannemann J, Carillo P, Höhne M, Hendriks JHM, Palacios N, Cross J, Selbig J, Stitt M (2004a) A robot-based platform to measure multiple enzyme activities in *Arabidopsis* using a set of cycling assays: comparison of changes of enzyme activities and transcript levels during diurnal cycles and in prolonged darkness. Plant Cell **16:** 3304–3325

Gibon Y, Bläsing OE, Palacios-Rojas N, Pankovic D, Hendriks JHM, Fisahn J, Hohne M, Gunther M, Stitt M (2004b) Adjustment of diurnal starch turnover to short days: depletion of sugar during the night leads to a temporary inhibition of carbohydrate utilization, accumulation of sugars and post-translational activation of ADP-glucose pyrophosphorylase in the following light period. Plant J **39:** 847–862

Gibon Y, Vigeolas H, Tiessen A, Geigenberger P, Stitt M (2002) Sensitive and high throughput metabolite assays for inorganic pyrophosphate, ADPGlc, nucleotide phosphates, and glycolytic intermediates based on a novel enzymic cycling assay. Plant J **30:** 221–235

Goldschmidt EE, Huber SG (1992) Regulation of photosynthesis by end-product accumulation in leaves of plants storing starch sucrose and hexose sugars. Plant Physiol **99:** 1443–1448

Gonzalez MC, Roitsch T, Cejudo FJ (2005) Circadian and developmental regulation of vacuolar invertase expression in petioles of sugar beet plants. Planta **222:** 386–395

Harbron S, Foyer C, Walker D (1981) The purification and properties of sucrose-phosphate synthase from spinach leaves: the involvement of this enzyme and fructose bisphosphatase in the regulation of sucrose biosynthesis. Arch Biochem Biophys **212:** 237–246

Huber JLA, Huber SC, Nielsen TH (1989) Protein phosphorylation as a mechanism for regulation of spinach leaf sucrose-phosphate synthase activity. Arch Biochem Biophys **270:** 681–690

Huber S (1989) Biochemical mechanism for regulation of sucrose accumulation in leaves during photosynthesis. Plant Physiol **91:** 656–662

Huber SC, Huber JL (1992) Role of sucrose-phosphate synthase in sucrose metabolism in leaves. Plant Physiol **99:** 1275–1278

Kasai M, Nakata H, Seino H, Kamata D, Tsukiyama T (2008) Effect of sink-limitation on leaf photosynthetic rate and related characteristics in soybean plants. Plant Prod Sci **11:** 223–227

Kingston-Smith AH, Walker RP, Pollock CJ (1999) Invertase in leaves: conundrum or control point? J Exp Bot **50:** 735–743

Klotke J, Kopka J, Gatzke N, Heyer AG (2004) Impact of soluble sugar concentrations on the acquisition of freezing tolerance in accessions of Arabidopsis thaliana with contrasting cold adaptation: evidence for a role of raffinose in cold acclimation. Plant Cell Environ **27:** 1395–1404

Knoke B, Textor S, Gershenzon J, Schuster S (2009) Mathematical modelling of aliphatic glucosinolate chain length distribution in *Arabidopsis thaliana* leaves. Phytochem Rev **8:** 39–51

Koch KE (1996) Carbohydrate-modulated gene expression in plants. Annu Rev Plant Physiol Plant Mol Biol **47:** 509–540

Kollist T, Moldau H, Rasulov B, Oja V, Rämma H, Hüve K, Jaspers P, Kangasjärvi J, Kollist H (2007) A novel device detects a rapid ozone-induced transient stomatal closure in intact Arabidopsis and its absence in abi2 mutant. Physiol Plant **129:** 796–803

Komor E (2000) Source physiology and assimilate transport: the interaction of sucrose metabolism, starch storage and phloem export in source leaves and the effects on sugar status in phloem. Aust J Plant Physiol **27:** 497–505

Krapp A, Hofmann B, Schafer C, Stitt M (1993) Regulation of the expression of *rbcs* and other photosynthetic genes by carbohydrates: a mechanism for the sink regulation of photosynthesis. Plant J **3:** 817–828

Laisk A, Eichelmann H, Oja V (2006) C-3 photosynthesis *in silico*. Photosynth Res **90:** 45–66

Le VQ, Samson G, Desjardins Y (2001) Opposite effects of exogenous sucrose on growth, photosynthesis and carbon metabolism of in vitro plantlets of tomato (*L. esculentum* Mill.) grown under two levels of irradiances and CO_2 concentration. J Plant Physiol **158:** 599–605

Lerchl J, Geigenberger P, Stitt M, Sonnewald U (1995) Impaired photoassimilate partitioning caused by phloem-specific removal of pyrophosphate can be complemented by a phloem-specific cytosolic yeast-derived invertase in transgenic plants. Plant Cell **7:** 259–270

Locke JCW, Kozma-Bognar L, Gould PD, Feher B, Kevei E, Nagy F, Turner MS, Hall A, Millar AJ (2006) Experimental validation of a predicted feedback loop in the multi-oscillator clock of *Arabidopsis thaliana*. Mol Syst Biol **2:** 59

Locke JCW, Millar AJ, Turner MS (2005) Modelling genetic networks with noisy and varied experimental data: the circadian clock in Arabidopsis thaliana. J Theor Biol **234:** 383–393

McCormick AJ, Cramer MD, Watt DA (2008) Regulation of photosynthesis by sugars in sugarcane leaves. J Plant Physiol **165:** 1817–1829

Moore B, Zhou L, Rolland F, Hall Q, Cheng W, Liu Y, Hwang I, Jones T, Sheen J (2003) Role of the Arabidopsis glucose sensor HXK1 in nutrient, light, and hormonal signaling. Science **300:** 332–336

Moore BD, Cheng SH, Rice J, Seemann JR (1998) Sucrose cycling, Rubisco expression, and prediction of photosynthetic acclimation to elevated atmospheric CO_2. Plant Cell Environ **21:** 905–915

Pettersson G, Ryde-Pettersson U (1988) A mathematical model of the Calvin photosynthesis cycle. Eur J Biochem **175:** 661–672

Poolman MG, Assmus HE, Fell DA (2004) Applications of metabolic modelling to plant metabolism. J Exp Bot **55:** 1177–1186

Poolman MG, Fell DA, Thomas S (2000) Modelling photosynthesis and its control. J Exp Bot **51:** 319–328

Riesmeier JW, Willmitzer L, Frommer WB (1994) Evidence for an essential role of the sucrose transporter in phloem loading and assimilate partitioning. EMBO J **13:** 1–7

Rizzi M, Baltes M, Theobald U, Reuss M (1997) *In vivo* analysis of metabolic dynamics in *Saccharomyces cerevisiae*. 2. Mathematical model. Biotechnol Bioeng **55:** 592–608

Roitsch T, Gonzalez M (2004) Function and regulation of plant invertases: sweet sensations. Trends Plant Sci **9:** 606–613

Schmidt H, Jirstrand M (2006) Systems biology toolbox for MATLAB: a computational platform for research in systems biology. Bioinformatics **22:** 514–515

Sergeeva LI, Keurentjes JJB, Bentsink L, Vonk J, van der Plas LHW, Koornneef M, Vreugdenhil D (2006) Vacuolar invertase regulates elongation of *Arabidopsis thaliana* roots as revealed by QTL and mutant analysis. Proc Natl Acad Sci USA **103:** 2994–2999

Smeekens S (2000) Sugar-induced signal transduction in plants. Annu Rev Plant Physiol Plant Mol Biol **51:** 49–81

Stelling J (2004) Mathematical models in microbial systems biology. Curr Opin Microbiol **7:** 513–518

Stessman D, Miller A, Spalding M, Rodermel S (2002) Regulation of photosynthesis during *Arabidopsis* leaf development in continuous light. Photosynth Res **72:** 27–37

Strand A, Hurry V, Gustafsson P, Gardestrom P (1997) Development of *Arabidopsis thaliana* leaves at low temperatures releases the suppression of photosynthesis and photosynthetic gene expression despite the accumulation of soluble carbohydrates. Plant J **12:** 605–614

Sturm A (1999) Invertases: primary structures, functions, and roles in plant development and sucrose partitioning. Plant Physiol **121:** 1–7

Sun JD, Okita TW, Edwards GE (1999) Modification of carbon partitioning, photosynthetic capacity, and O_2 sensitivity in Arabidopsis plants with low ADP-glucose pyrophosphorylase activity. Plant Physiol **119:** 267–276

Tang X, Ruffner HP, Scholes JD, Rofle SA (1996) Purification and characterization of soluble invertases from leaves of *Arabidopsis thaliana*. Planta **198:** 17–23

Theobald U, Mailinger W, Baltes M, Rizzi M, Reuss M (1997) *In vivo* analysis of metabolic dynamics in *Saccharomyces cerevisiae*. 1. Experimental observations. Biotechnol Bioeng **55:** 305–316

Uys L, Botha FC, Hofmeyr JS, Rohwer JM (2007) Kinetic model of sucrose accumulation in maturing sugarcane culm tissue. Phytochemistry **68:** 2375–2392

Vaz AIF, Vicente LN (2007) A particle swarm pattern search method for bound constrained global optimization. J Glob Optim **39:** 197–219

Wiese A, Gröner F, Sonnewald U, Deppner H, Lerchl J, Hebbeker U, Flügge U, Weber A (1999) Spinach hexokinase I is located in the outer envelope membrane of plastids. FEBS Lett **461:** 13–18

Yu XY, Wang XF, Zhang WQ, Qian TT, Tang GM, Guo YK, Zheng CC (2008) Antisense suppression of an acid invertase gene (*MAI1*) in muskmelon alters plant growth and fruit development. J Exp Bot **59:** 2969–2977

Yuan JS, Galbraith DW, Dai SY, Griffin P, Stewart CN (2008) Plant systems biology comes of age. Trends Plant Sci **13:** 165–171